Pharmaceutical Sciences and Drug Design
ISSN: 3062-4428
2024, Volume 4, Page No: 168-181

Available online at: www.galaxypub.co/page/journals

Galaxy Publication

Protective Effects of Sichen Formula on LPS-Induced Acute Lung Injury via Modulation of TLR4 Signaling Pathways

Xiao Li[1]*, Wen Zhang[1]

[1]Department of Pharmacognosy, Faculty of Pharmacy, Peking University, Beijing, China.

*** E-mail** ✉ xiao.li.cn@gmail.com

Received: 09 August 2024; **Revised:** 14 November 2024; **Accepted:** 18 November 2024

ABSTRACT

Sichen (SC) formula, a well-known Tibetan medicinal preparation, has been traditionally applied to treat respiratory ailments in Tibet due to its anti-inflammatory potential. This study aimed to systematically investigate its anti-inflammatory effects and the molecular mechanisms involved. The chemical profile of SC was analyzed using HPLC. An acute lung injury (ALI) model in mice was established by intratracheal administration of lipopolysaccharide (LPS), with subsequent collection of bronchoalveolar lavage fluid (BALF) and lung tissues for analysis. RAW264.7 macrophages were also exposed to LPS in vitro. Inflammatory cytokine levels were measured by ELISA, while protein expression and localization were evaluated using Western blot, immunohistochemistry, and immunofluorescence for NF-κB, AP-1, and IRF3.In LPS-induced ALI mice, SC significantly reduced BALF levels of TNF-α, IL-6, IL-1β, MCP-1, MIP-1α, and RANTES, and limited macrophage infiltration. SC treatment also decreased the expression of CD68, TLR4, and phosphorylated p65 in lung tissues. In RAW264.7 macrophages, SC up to 400 μg/mL did not affect viability but dose-dependently suppressed inflammatory mediators including nitric oxide, prostaglandin E2, and multiple cytokines. SC inhibited the activation of key signaling proteins, including iNOS, COX-2, p-p38, p-JNK, p-ERK, p-TBK1, p-IKKα/β, p-IκB, p-p65, p-c-Jun, and p-IRF3, and blocked nuclear translocation of NF-κB, AP-1, and IRF3.SC exerts potent anti-inflammatory effects in both LPS-induced ALI mice and LPS-stimulated macrophages, likely through modulation of the TLR4 signaling pathway. These findings provide experimental evidence supporting the therapeutic application of SC in respiratory inflammatory disorders.

Keywords: Sichen formula, Acute lung injury, Macrophages, Lipopolysaccharide, TLR4 pathway

How to Cite This Article: Li X, Zhang W. Protective Effects of Sichen Formula on LPS-Induced Acute Lung Injury via Modulation of TLR4 Signaling Pathways. Pharm Sci Drug Des. 2024;4:168-81. https://doi.org/10.51847/fOYQ5k3OOE

Introduction

Acute lung injury (ALI) and its severe form, acute respiratory distress syndrome (ARDS), are characterized by extensive lung inflammation, involving damage to the alveolar epithelium and endothelium, platelet deposition, and leukocyte aggregation [1]. ALI can rapidly progress to respiratory failure and is associated with high mortality. Its etiology includes sepsis, pneumonia, aspiration, and trauma [2, 3]. ALI/ARDS remains a leading cause of morbidity in intensive care units, with hospital mortality rates around 40% [4]. Current management primarily relies on supportive care and pharmacologic interventions, with mechanical ventilation being essential for maintaining oxygenation and carbon dioxide removal, as no definitive pharmacological therapy exists [5]. Corticosteroids are commonly used to improve gas exchange and hemodynamic stability; however, long-term use carries risks of adverse effects such as hyperglycemia and infections [6]. Therefore, safe and effective therapeutic options to halt or reverse ALI progression are urgently needed.

Macrophages are key players in innate immunity, responsible for clearing inhaled particles and pathogens, and they contribute significantly to ALI pathogenesis [7]. These cells recognize endogenous danger signals, such as lipopolysaccharide (LPS) from Gram-negative bacteria, via Toll-like receptor 4 (TLR4) [8]. TLR4 activation triggers intracellular signaling cascades, leading to phosphorylation of the IκB and IKK complex and subsequent nuclear translocation of NF-κB [9]. Additional kinases, including JNK, p38 MAPK, and ERK, activate AP-1,

while TLR4 also phosphorylates TBK1, which in turn activates IRF3, promoting its dimerization and nuclear translocation [10, 11]. These transcription factors drive the production of pro-inflammatory cytokines and chemokines, amplifying lung injury. Hence, inhibition of TLR4 signaling represents a promising therapeutic approach for ALI.

Sichen (SC) formula, a traditional Tibetan medicine, consists of Radix Phlomii, Rhizoma Bergeniae, Herba Artemisiae scoparae, and Radix Glycyrrhizae in a 1.5:1:2:2 ratio. It has long been used to clear heat, relieve cough, and reduce phlegm [12]. Clinically, SC has been employed to treat respiratory conditions, including infections, chronic bronchitis, and asthma [13, 14]. Despite its therapeutic use, limited research has examined SC's effects on ALI, and the mechanisms underlying its action remain unclear. In this study, we established an LPS-induced ALI mouse model to evaluate SC's anti-inflammatory properties and utilized LPS-stimulated RAW264.7 macrophages to investigate the molecular mechanisms involved.

Materials and Methods

Materials

Lipopolysaccharide (LPS, Escherichia coli O55:B5), MTT, modified Griess reagent, and Wright stain solution were obtained from Sigma-Aldrich (St. Louis, MO, USA). Penicillin–streptomycin solution was purchased from Caisson Labs (Smithfield, UT, USA), and fetal bovine serum (FBS) from Biological Industries (Beth-Haemek, Israel). Dexamethasone was sourced from Tianjin Lisheng Pharmaceutical Co., Ltd., and DMEM from Corning Cellgro (Manassas, VA, USA). ELISA kits for TNF-α, IL-6, IL-1β, MIP-1α, MCP-1, and RANTES were purchased from Thermo Fisher Scientific (San Diego, CA, USA), and a PGE2 ELISA kit from Enzo Life Sciences (Exeter, UK).

Primary antibodies against CD68, TLR4, GAPDH, and phospho-NF-κB p65 for immunohistochemistry were obtained from Santa Cruz Biotechnology (Santa Cruz, CA, USA). Antibodies against IKKβ and Sp1 were from Proteintech (Rosemont, USA), while anti-IRF3, iNOS, anti-mouse IgG, and HRP-conjugated secondary antibodies were purchased from Abcam (Cambridge, UK). Phospho-IRF3 antibody was obtained from ABNOVA (Taiwan, China). Antibodies for NF-κB p65, phospho-p65, c-Jun, phospho-c-Jun, COX-2, IκBα, phospho-IκBα, phospho-IKKα/β, ERK, phospho-ERK, JNK, phospho-JNK, p38 MAPK, phospho-p38, TBK1, phospho-TBK1, β-actin, anti-rabbit IgG-HRP, and Alexa Fluor 488 secondary antibody were supplied by Cell Signaling Technology (Boston, MA, USA). Stripping buffer was purchased from Solarbio (Beijing, China). Reference standards including chlorogenic acid, bergenin, and ammonium glycyrrhizate were provided by the National Institutes for Food and Drug Control.

Preparation of Sichen (SC) formula

The herbal components of SC, including Radix Phlomii, Rhizoma Bergeniae, Herba Artemisiae scoparae, and Radix Glycyrrhizae, were obtained from the Tibetan Traditional Medical College and authenticated by Prof. Ci-Ren Nima. Voucher specimens were deposited at the Department of Pharmacology, School of Chinese Medicine, Beijing University of Chinese Medicine. The air-dried crude herbs (Radix Glycyrrhizae: Herba Artemisiae scoparae: Radix Phlomii: Rhizoma Bergeniae = 4:4:3:2, totaling 6500 g) were extracted three times via reflux with eightfold volumes of water for 1.5 h per extraction. The combined extracts were concentrated under reduced pressure at 90°C and vacuum-dried at 70°C to obtain SC powder.

HPLC characterization of SC

SC powder was sonicated in 50% methanol for 30 min and filtered prior to analysis. The levels of bergenin, chlorogenic acid, and ammonium glycyrrhizate were quantified using a Shimadzu LC-20A HPLC system (Shimadzu, Japan) equipped with an Acclaim™ 120 C18 column (4.6 mm × 250 mm, 5 μm; Thermo Fisher Scientific, USA) at 20°C. The mobile phase consisted of acetonitrile (solvent A) and 0.1% phosphoric acid water (solvent B) using a gradient program (0–16 min, 4–8% A; 16–30 min, 8–9% A; 30–50 min, 9–16% A; 50–70 min, 16–17% A; 70–73 min, 17–20% A; 73–93 min, 20–28% A; 93–105 min, 28–43% A; 105–120 min, 43–50% A) at 0.8 mL/min. Detection was performed at 254 nm with a 10 μL injection volume.

Molecular docking

The crystal structure of TLR4 (PDB ID: 2Z66) was retrieved from the Protein Data Bank. Ligands and water molecules were removed using PyMOL. Structures of bergenin, chlorogenic acid, and ammonium glycyrrhizate (with ammonium removed) were obtained from PubChem and prepared with hydrogen atoms using AutoDock Vina. Rigid docking simulations were conducted with AutoDock Vina, and hydrogen bonds and bond lengths were analyzed and visualized using PyMOL [15].

Animal model of ALI

Male BALB/c mice (18–22 g) were purchased from SPF Biotechnology Co., Ltd (Beijing, China) and maintained at the Department of Pharmacology, School of Chinese Materia Medica, Beijing University of Chinese Medicine. Animals were housed under standard conditions (12 h light/dark cycle, 20–22°C, 50–55% humidity) with ad libitum access to food and water. All experiments were approved by the University Committee on Research Practice and followed NIH guidelines for animal care. Mice were randomly assigned to six groups (n = 10 each): (1) control, (2) model, (3) SC 2.7 g/kg/d, (4) SC 5.4 g/kg/d, (5) SC 10.8 g/kg/d, and (6) dexamethasone 1.8 mg/kg/d. Treatments were administered intragastrically for five consecutive days, while control and model groups received PBS. Eighteen hours after the final dose, mice were anesthetized with sodium pentobarbital (50 mg/kg) and given intratracheal LPS (125 μg/mouse) or PBS. After 18 h, bronchoalveolar lavage fluid (BALF) was collected by instilling 0.3 mL PBS into the right lung three times. BALF was centrifuged at 2000 ×g for 8 min at 4°C; the cell pellet was resuspended for total and differential cell counts, while supernatants were stored at −80°C. Left lung tissues were collected for subsequent analyses.

Histological examination

Lung tissue samples were fixed in 10% neutral buffered formalin, embedded in paraffin, and sectioned at 5 μm. Sections were stained with hematoxylin and eosin and examined under a Nikon Eclipse Ts2R microscope at 200× magnification. Pathological scoring included goblet cell hyperplasia, hemorrhage, and inflammatory cell infiltration (0–4 scale), with cumulative scores representing total tissue injury [16]. Ten samples per group were evaluated.

Immunohistochemistry

Paraffin lung sections were deparaffinized, rehydrated, and subjected to citric acid antigen retrieval for 45 min. After hydrogen peroxide blocking, slides were incubated with primary antibodies against CD68, TLR4, or phospho-p65 for 2 h at room temperature, followed by biotinylated goat anti-mouse IgG for 20 min and DAB chromogenic detection. Sections were counterstained with hematoxylin, dehydrated, and imaged. Positive staining areas were quantified with Image-Pro Plus 5.1 (three images per slice, ten slices per group).

Cell culture and viability assay

RAW264.7 macrophages were maintained in DMEM with 10% FBS and antibiotics at 37°C under 5% CO2. Cells were seeded at 6 × 10^3 cells/well in 96-well plates and treated with SC (6.25–400 μg/mL) ± LPS (1 μg/mL) for 24 h. Cell viability was determined using MTT assay, measuring absorbance at 570 nm. Six replicates per condition were performed.

Measurement of inflammatory mediators

RAW264.7 cells were seeded at 2 × 10^5 cells/well in 24-well plates, pretreated with SC (50–400 μg/mL) for 1 h, and exposed to LPS (1 μg/mL) for 24 h. Levels of TNF-α, IL-6, IL-1β, MCP-1, MIP-1α, RANTES, and PGE2 were quantified using ELISA kits, while nitric oxide was measured using Griess reagent. Four replicates were used per condition; BALF samples (n = 7–8 per group) were analyzed similarly.

Western blot analysis

RAW264.7 cells or lung tissue samples were lysed in RIPA buffer, and nuclear/cytoplasmic fractions were separated using a nuclear extraction kit. Proteins (40 μg) were separated by 10% SDS-PAGE, transferred to PVDF membranes, and blocked with 5% milk in TBST. Membranes were incubated overnight with primary antibodies, followed by HRP-conjugated secondary antibodies for 1 h. Bands were visualized using enhanced chemiluminescence and quantified with ImageJ, normalized to β-actin, GAPDH, or Sp1. Six lung tissue samples and five cell samples per group were analyzed [17].

Immunofluorescence staining

To evaluate the nuclear translocation of key transcription factors NF-κB, AP-1, and IRF3, immunofluorescence staining was performed following previously established protocols [18]. RAW264.7 cells (1 × 10^4) were seeded onto chamber slides for 24 hours. Cells were pretreated with SC (200 or 400 μg/mL) for 1 hour, followed by LPS stimulation (1 μg/mL) for 30 minutes. Cells were then fixed with 4% formaldehyde in PBS for 15 minutes, permeabilized with 0.25% Triton X-100 at 37°C for 30 minutes, and blocked with 2% BSA for 1 hour. Primary antibodies were applied overnight at 4°C, followed by incubation with fluorescently labeled goat anti-rabbit secondary antibodies for 1 hour at room temperature, with three washes using PBST. Nuclear DNA was stained with DAPI (YESEN, Shanghai, China). Imaging was performed on a Nikon A1R confocal microscope. Quantitative analysis of nuclear fluorescence was carried out on 50 cells per group using ImageJ software. Nuclear regions were defined as regions of interest (ROIs), and mean fluorescence intensity within these ROIs was calculated to assess transcription factor localization.

Statistical analysis

All measurements are presented as mean ± SEM. Statistical analyses were conducted using GraphPad Prism 9.0. Normality was assessed with the Shapiro–Wilk test for sample sizes >5, or QQ plots for $n \leq 5$. For normally distributed data with equal variances, one-way ANOVA was applied. Datasets showing unequal variances were analyzed using Brown-Forsythe and Welch ANOVA tests. Non-normally distributed data were analyzed with the Kruskal–Wallis test. Differences were considered significant at $p < 0.05$.

Results and Discussion

Quality control and molecular docking of sichen formula

HPLC profiling confirmed the presence of three major active constituents in SC: bergenin from Rhizoma Bergeniae, chlorogenic acid from Herba Artemisiae scoparae, and ammonium glycyrrhizate from Radix Glycyrrhizae [19–21]. Quantitative analysis revealed concentrations of 36.8 mg/g, 14.34 mg/g, and 22.46 mg/g for bergenin, chlorogenic acid, and ammonium glycyrrhizate, respectively **(Figures 1a–1d)**. Molecular docking studies indicated that these components interact with TLR4 with binding energies of −4.46, −2.87, and −3.62 kcal/mol, respectively **(Figure 1e)**. Bergenin formed hydrogen bonds with residues GLN-436, HIS-566, ASP-596, SER-589, and LEU-56, while chlorogenic acid engaged SER-39, LYS-62, GLN-562, and GLU-536. Ammonium glycyrrhizate interacted via ASP-395 and LYS-388. These docking results suggest that SC components can directly bind TLR4, implying a potential mechanism for SC-mediated suppression of TLR4-driven inflammatory pathways.

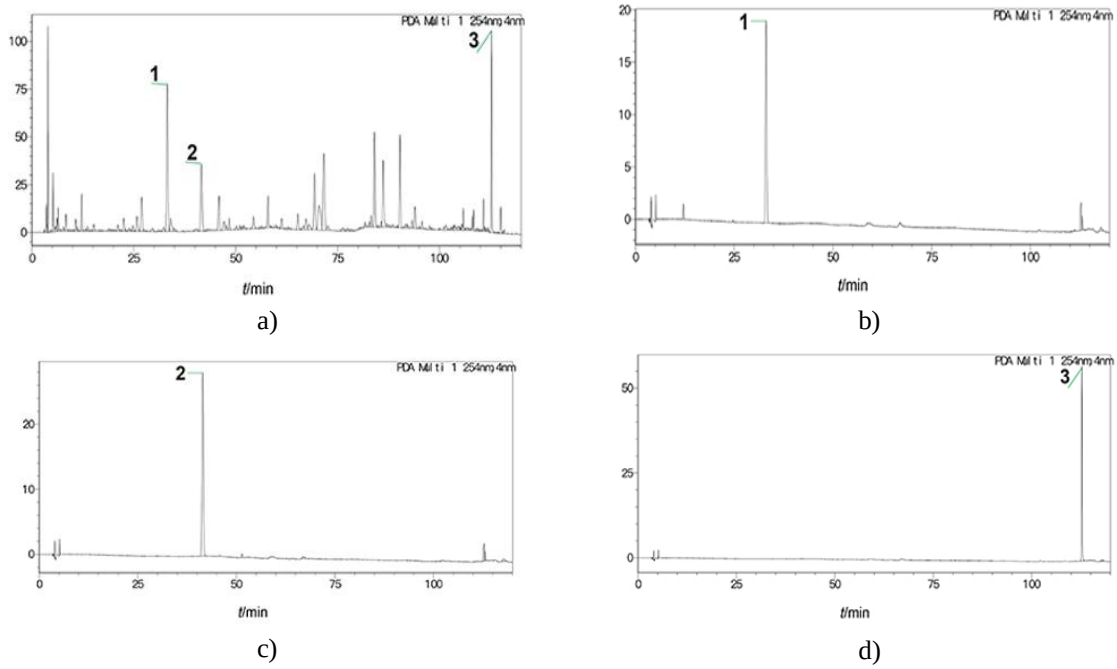

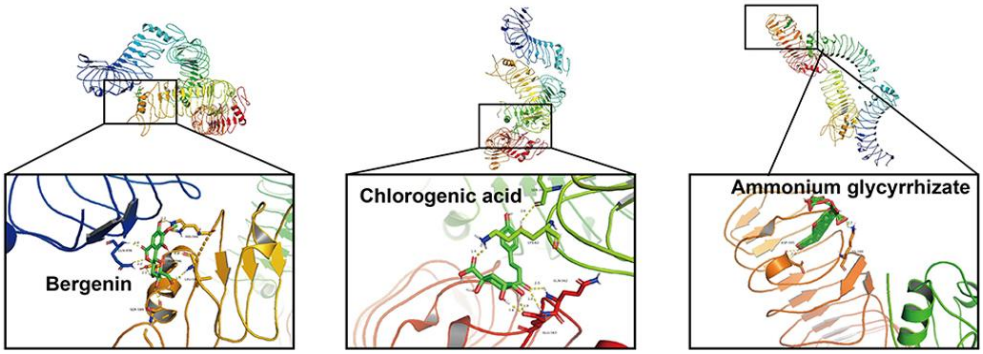

e)

Figure 1. HPLC Profiling of SC Components and Their Interaction with TLR4

HPLC analysis of SC dissolved in 50% methanol revealed the presence of three major bioactive constituents: bergenin, chlorogenic acid, and ammonium glycyrrhizate, as shown in panels a–d. Peaks 1, 2, and 3 correspond to bergenin, chlorogenic acid, and ammonium glycyrrhizate, respectively. Molecular docking studies (e) were performed using AutoDock Vina with the crystal structure of TLR4 (PDB code: 2Z66), and the interactions were visualized in PyMOL. Hydrogen bonding interactions are indicated by yellow dashed lines.

SC treatment mitigates LPS-Induced lung injury and inflammatory responses in mice

To evaluate the protective effects of SC against ALI, an LPS-induced mouse model was established. Histopathological examination revealed that LPS exposure caused extensive infiltration of inflammatory cells, thickening of alveolar walls, and disruption of alveolar epithelial tight junctions. Pretreatment with SC substantially alleviated these histological abnormalities, as reflected by lower pathological scores compared to the LPS-only group **(Figure 2a).**

LPS administration significantly increased total immune cell counts in BALF, promoting the recruitment of macrophages and neutrophils to the bronchoalveolar spaces. SC at 10.8 g/kg effectively reduced macrophage infiltration induced by LPS **(Figure 2b)**. Consistent with these findings, immunohistochemistry demonstrated an elevated CD68-positive area in lung tissues following LPS challenge, which was markedly reduced in SC-treated mice, indicating diminished macrophage accumulation **(Figure 2c).**

Furthermore, SC treatment suppressed the LPS-induced release of pro-inflammatory cytokines (TNF-α, IL-1β, IL-6) and chemokines (MCP-1, MIP-1α, RANTES) in BALF **(Figure 2d)**. Western blot and immunohistochemical analyses revealed that SC also downregulated the expression of TLR4 and phosphorylated NF-κB p65 in lung tissues from LPS-exposed mice **(Figure 3)**, suggesting that SC may exert its anti-inflammatory effects by modulating the TLR4 signaling pathway.

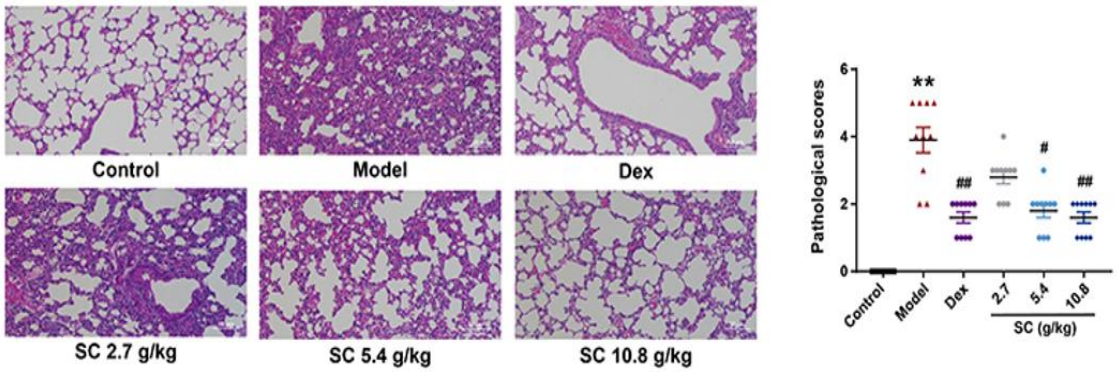

a)

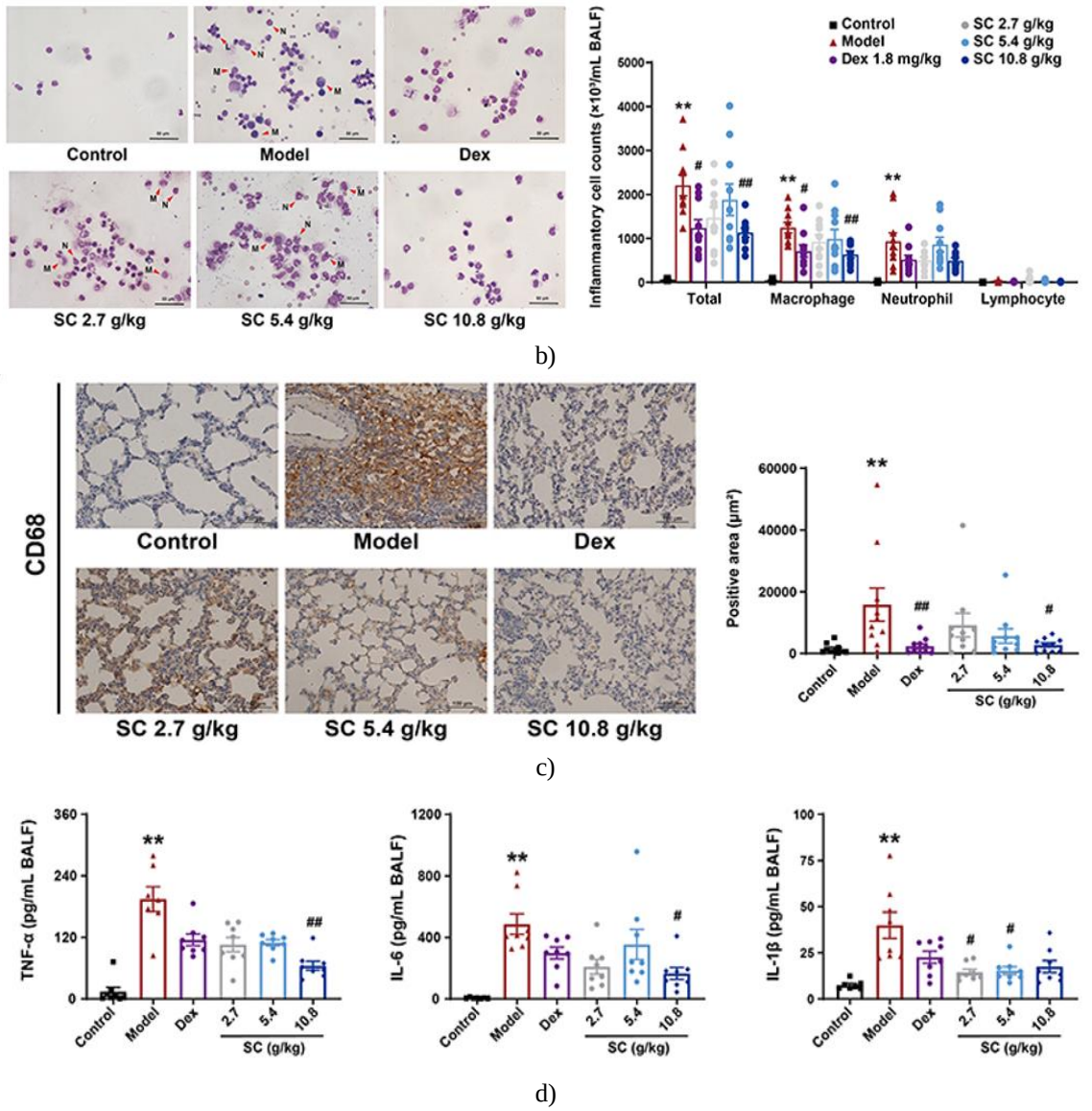

Figure 2. SC reduces lung inflammation in LPS-challenged mice.

BALB/c mice received oral pretreatment for five days with SC at doses of 2.7, 5.4, or 10.8 g/kg, or dexamethasone (1.8 mg/kg), followed by intratracheal LPS administration (125 μg/mouse) for 18 hours.

(a) Representative hematoxylin and eosin-stained lung sections. Tissue damage, including alveolar thickening, inflammatory infiltration, and structural disruption, was scored semi-quantitatively (right panel, n = 10/group; Kruskal–Wallis with Dunn's post hoc test).

(b) Wright-stained BALF cytospin preparations. Total cell numbers were determined by hemocytometer (n = 10/group; Brown-Forsythe and Welch ANOVA with Dunnett's T3 test). Differential counts of macrophages, neutrophils, and lymphocytes were assessed under 400× magnification (n = 10/group). Red arrowheads highlight macrophages (M), neutrophils (N), and lymphocytes (L).

(c) Immunohistochemical detection of CD68 in lung tissue. The area of CD68-positive staining was quantified to reflect macrophage accumulation (n = 10/group; Kruskal–Wallis with Dunn's post hoc).

(d) Concentrations of cytokines (TNF-α, IL-6, IL-1β) and chemokines (MCP-1, MIP-1α, RANTES) in BALF measured by ELISA (n = 7–8/group). Statistical tests: Kruskal–Wallis for TNF-α, IL-6, IL-1β, MCP-1, and MIP-1α; one-way ANOVA with Fisher's LSD for RANTES.

Data are shown as mean ± SEM. **p < 0.01 compared to control; #p < 0.05, ##p < 0.01 compared to LPS model group.

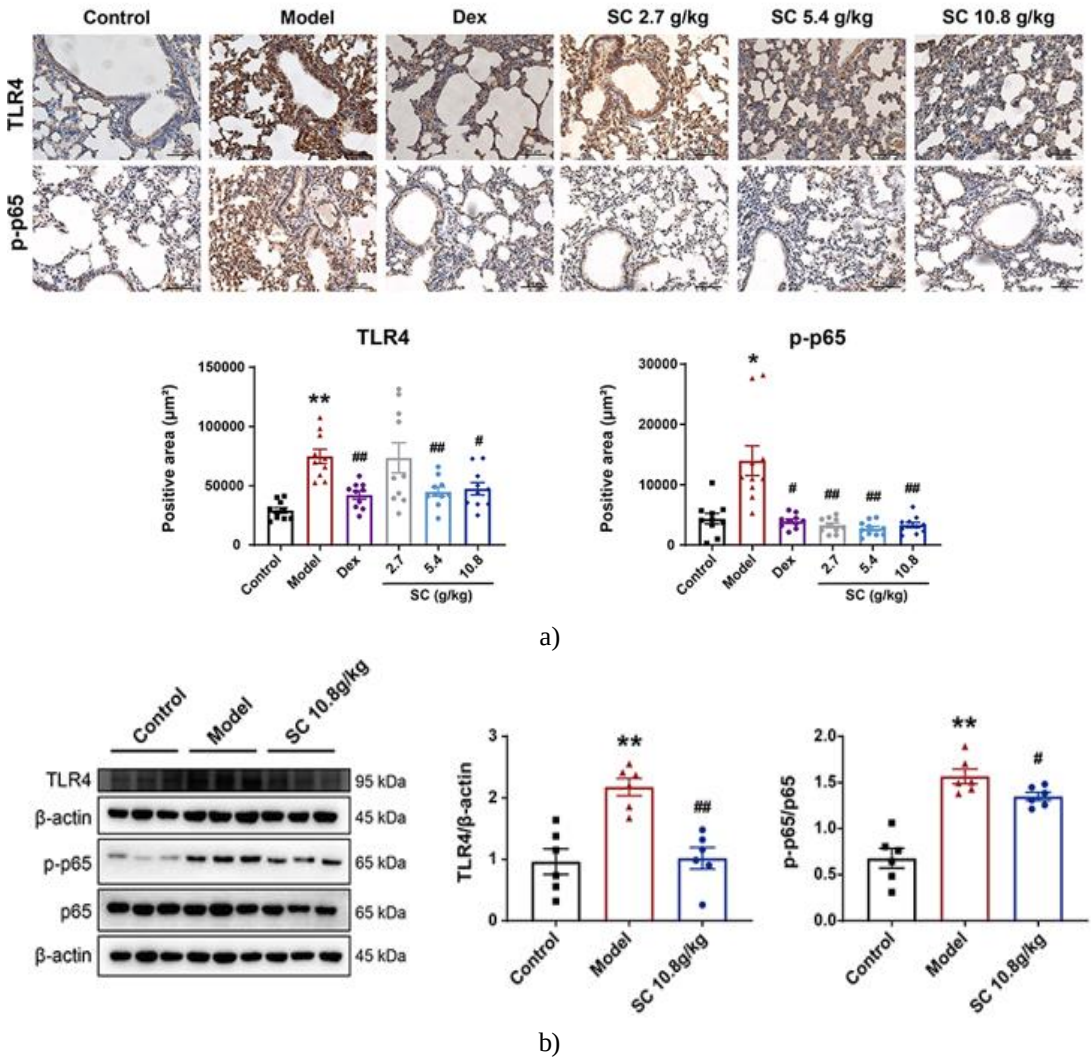

Figure 3. SC suppresses TLR4 and p-p65 signaling in LPS-induced ALI.

(a) Lung tissue sections from LPS-challenged mice were stained for TLR4 and phosphorylated p65. Quantitative analysis of positively stained areas was conducted (n = 10/group; TLR4, Brown-Forsythe and Welch ANOVA; p-p65, Kruskal–Wallis test).

(b) Western blot analysis of lung tissue lysates showing TLR4 and phospho-p65 levels, with β-actin as the loading control. Densitometry data are presented as mean ± SEM (n = 6/group, unpaired two-tailed t-test). Significance: *p < 0.05, **p < 0.01 versus control; #p < 0.05, ##p < 0.01 versus LPS-only group

SC reduces inflammatory mediator production in LPS-stimulated RAW264.7 macrophages

To examine SC's effect on macrophage-mediated inflammation, RAW264.7 cells were exposed to LPS in the presence or absence of SC. Cell viability assays indicated that SC at concentrations up to 400 μg/mL did not impair macrophage survival, confirming its non-toxic profile **(Figure 4a)**. Consequently, SC concentrations ranging from 50 to 400 μg/mL were selected for functional studies.

Exposure to LPS led to a pronounced increase in nitric oxide (NO) and prostaglandin E2 (PGE2). Treatment with SC effectively reduced the production of both mediators in a dose-dependent manner (**Figures 4b and 4c)**. Similarly, SC lowered the LPS-induced upregulation of iNOS and COX-2, the key enzymes responsible for NO and PGE2 synthesis **(Figure 4d).**

In addition, SC markedly decreased the release of IL-6 and chemokines, including MCP-1, MIP-1α, and RANTES, following LPS stimulation. TNF-α levels were reduced by SC, although the decrease was not statistically significant **(Figure 4e)**. These results indicate that SC can dampen LPS-triggered inflammatory responses in macrophages without affecting cell viability.

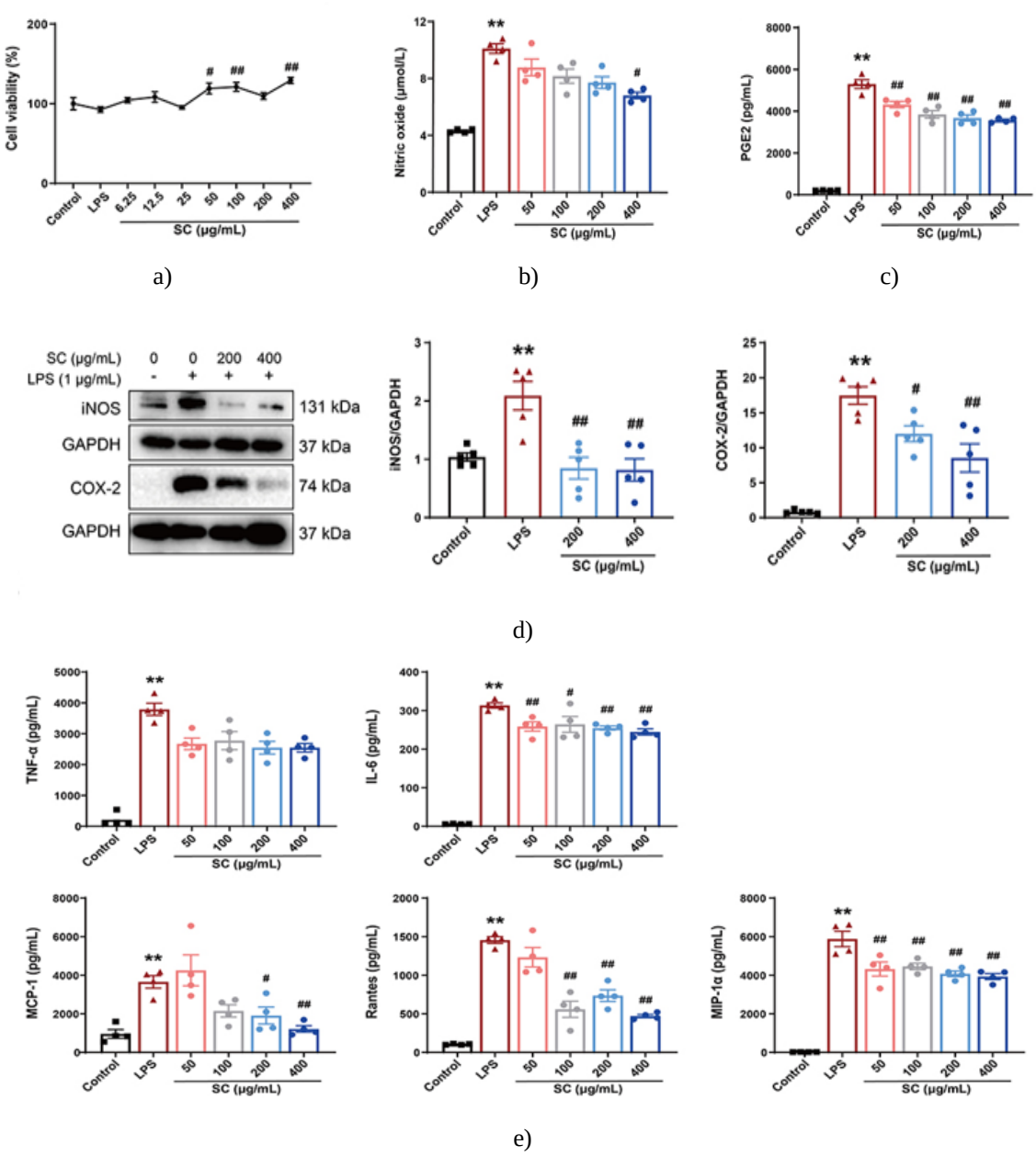

Figure 4. SC attenuates inflammatory mediator release in RAW264.7 macrophages stimulated with LPS RAW264.7 cells were exposed to SC (50–400 μg/mL) for 1 hour prior to stimulation with 1 μg/mL LPS for 24 hours. SC showed no cytotoxicity at concentrations up to 400 μg/mL (n = 6), allowing assessment of its anti-inflammatory effects.

SC treatment significantly reduced the production of nitric oxide and prostaglandin E2 in a dose-dependent manner, corresponding to a decrease in iNOS and COX-2 protein levels (n = 4–5). Pro-inflammatory cytokines and chemokines, including IL-6, MCP-1, MIP-1α, and RANTES, were also suppressed after SC exposure. Although TNF-α secretion was slightly lowered, this reduction was not statistically significant compared to LPS-only treated cells.

SC modulates TLR4 signaling to limit inflammation in LPS-stimulated macrophages

Given the central role of TLR4 in driving inflammatory responses, the impact of SC on this pathway was examined. LPS stimulation strongly activated key transcription factors, including NF-κB (p65), AP-1 (c-Jun), and IRF3, as shown by increased phosphorylation and nuclear translocation. SC pretreatment dose-dependently inhibited these activation events.

Additionally, LPS induced phosphorylation of MAPK pathway proteins ERK, p38, and JNK, as well as upstream regulators IκBα, IKKα/β, and TBK1. SC effectively suppressed these phosphorylation events, indicating that it can block both upstream and downstream components of the TLR4-mediated signaling cascade. Collectively, these results suggest that SC mitigates inflammatory responses by interfering with TLR4-driven intracellular signaling in macrophages.

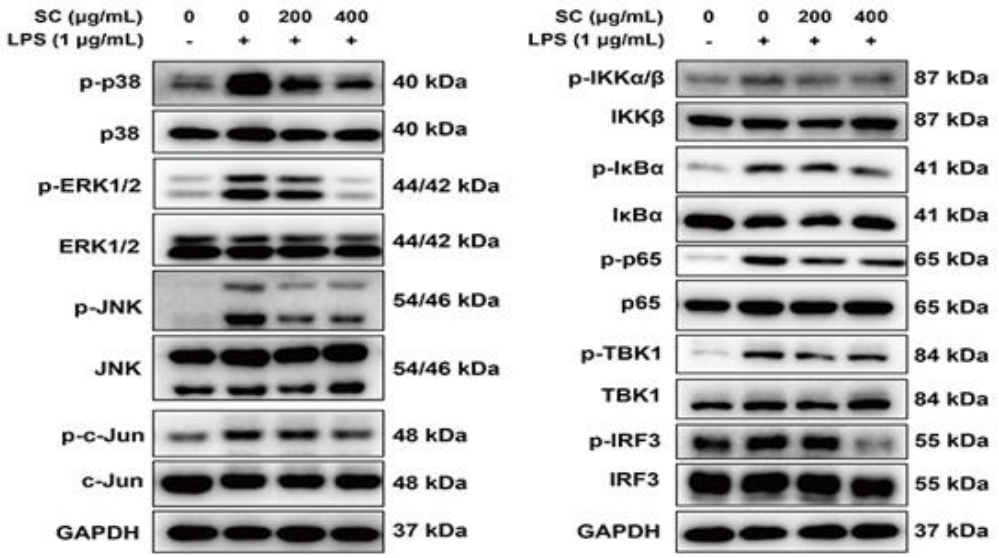

a)

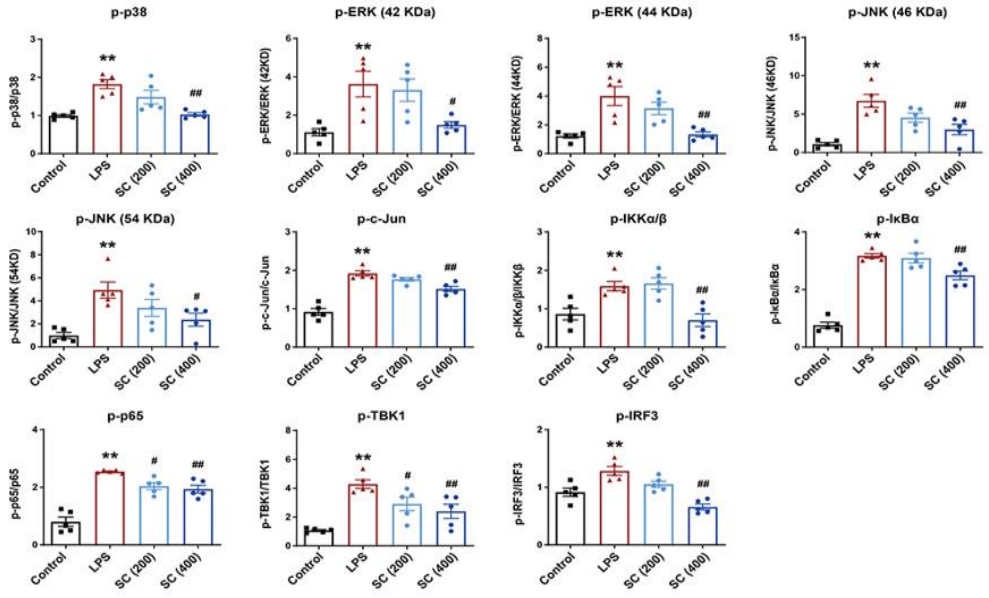

b)

Figure 5. SC suppresses TLR4-mediated signaling in LPS-activated RAW264.7 macrophages RAW264.7 cells were pretreated with SC at 200 or 400 μg/mL for 1 hour, followed by LPS stimulation (1 μg/mL) for 30 minutes. Western blot analysis revealed that LPS markedly increased phosphorylation of key signaling proteins, including MAPKs (p38, JNK, ERK), AP-1 (c-Jun), NF-κB pathway components (IKK, IκBα, p65), TBK1, and IRF3. Pretreatment with SC dose-dependently reduced phosphorylation of these proteins, while total protein levels remained largely unchanged (n = 5). These results indicate that SC can interfere with both upstream and downstream elements of the TLR4 signaling cascade.

SC prevents nuclear translocation of NF-κB, AP-1, and IRF3

The nuclear migration of transcription factors NF-κB, AP-1, and IRF3 is essential for initiating pro-inflammatory gene expression in response to LPS. Immunofluorescence imaging showed that LPS triggered pronounced nuclear

accumulation of p65, c-Jun, and IRF3, whereas SC pretreatment markedly diminished this nuclear localization in a concentration-dependent manner **(Figure 6a)**. Consistently, Western blot analysis of nuclear and cytoplasmic fractions confirmed that SC reduced nuclear levels of p65, c-Jun, and IRF3 without affecting their cytoplasmic expression **(Figure 6b)**. Collectively, these findings suggest that SC attenuates inflammatory responses by preventing nuclear translocation of key transcription factors downstream of TLR4.

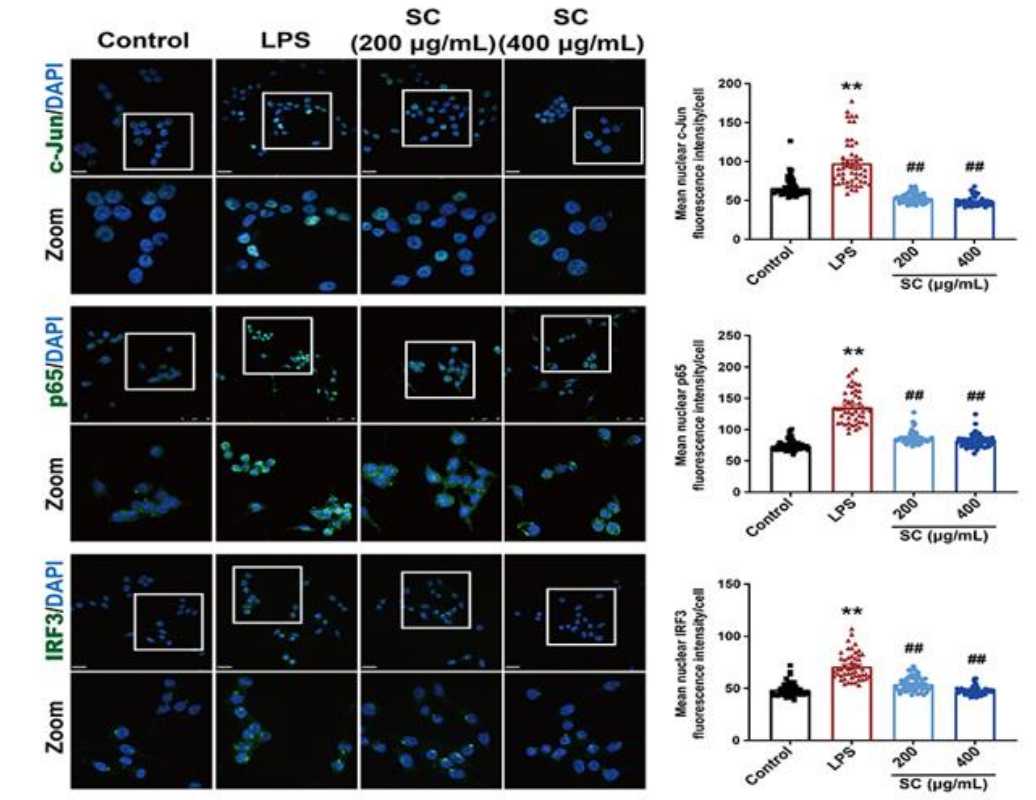

a)

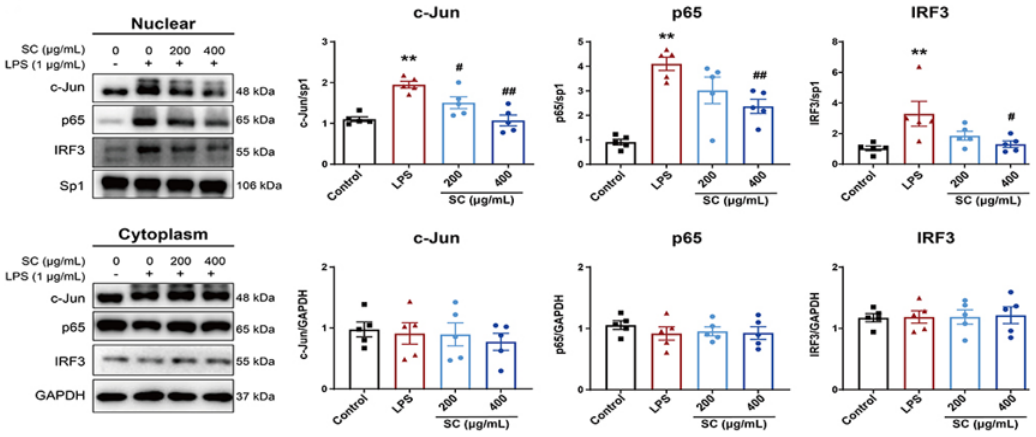

b)

Figure 6. SC inhibits nuclear translocation of NF-κB, AP-1, and IRF3 in LPS-treated RAW264.7 macrophages

RAW264.7 cells were pretreated with SC at 200 or 400 μg/mL for 1 hour before exposure to 1 μg/mL LPS for 30 minutes. (a) Immunofluorescence staining revealed that LPS promoted nuclear accumulation of NF-κB subunit p65, AP-1 subunit c-Jun, and IRF3. SC pretreatment reduced the nuclear localization of these transcription factors in a dose-dependent manner. Scale bars: 17 μM for c-Jun and IRF3, 50 μM for p65. Quantitative analysis was performed on 50 cells per group using ImageJ (Kruskal–Wallis test with Dunn's post hoc test). (b) Western blotting of nuclear and cytoplasmic fractions confirmed that SC reduced the

nuclear levels of p65, c-Jun, and IRF3 without altering their cytoplasmic abundance. Sp1 and GAPDH were used as loading controls. Relative protein expression is shown (n = 5, one-way ANOVA with Dunnett's post hoc test). Data are expressed as mean ± SEM. **p < 0.01 vs. control; #p < 0.05, ##p < 0.01 vs. LPS

ALI represents a spectrum of pulmonary alterations triggered by diverse forms of lung injury, often leading to poor clinical outcomes and, in severe cases, life-threatening respiratory failure [3]. Current pharmacological treatments for ALI remain unsatisfactory due to significant side effects and high cost. Traditional Tibetan medicines or formulas may offer promising sources of safe and effective therapeutic agents [22], particularly for respiratory disorders such as ALI [23]. In this study, we demonstrated that SC, a classical Tibetan herbal prescription used for acute and chronic respiratory illnesses, mitigated LPS-induced inflammatory responses both in vivo and in vitro. Several constituents of SC—such as bergenin, chlorogenic acid, and monoammonium glycyrrhizinate—have previously been reported to possess anti-inflammatory properties [24–26]. Our docking analysis also showed that these compounds can bind to TLR4, suggesting that the anti-inflammatory activity of SC may be partly attributable to these bioactive components. Further investigations will focus on identifying the primary active ingredients responsible for SC's anti-inflammatory effects.

Alveolar macrophages are central to the release of inflammatory mediators that recruit neutrophils, monocytes, and other immune effector cells into the lung, especially during acute and chronic respiratory infections, ultimately causing alveolar epithelial damage and impaired lung function [27]. Our preliminary findings indicated that SC markedly reduced airway hyperresponsiveness in rats with chronic bronchitis (data not shown), implying a potential protective effect on lung performance. Using the LPS-induced ALI mouse model, we observed that SC significantly decreased the levels of inflammatory cytokines (TNF-α, IL-6, IL-1β) and chemokines (MCP-1, MIP-1α, RANTES) in BALF. Histological evaluation with HE and Wright staining also revealed that SC treatment reduced alveolar inflammatory cell infiltration, particularly macrophages. Moreover, SC administration reduced CD68 expression, a macrophage-specific surface marker [28], further supporting its role in suppressing macrophage activation following LPS exposure. These findings suggest that the anti-inflammatory mechanism of SC is closely linked to its inhibitory effects on macrophage activation.

TLR4 signaling, activated by ligands such as LPS, plays a major role in the onset and progression of ALI [29]. This pathway triggers two downstream cascades—MyD88-dependent and TRIF-dependent—both of which lead to the nuclear activation of NF-κB, AP-1, and IRF3, driving the transcription of pro-inflammatory genes including TNF-α, IL-6, IL-1β, MCP-1, MIP-1α, and RANTES [29]. In our LPS-induced ALI model, SC decreased TLR4 recruitment and NF-κB phosphorylation, indicating that SC may interfere with TLR4-mediated signaling. To verify this, we tested SC in RAW264.7 macrophages. Consistent with the in vivo findings, SC inhibited LPS-induced release of inflammatory mediators—NO, PGE2, IL-6, MCP-1, MIP-1α, and RANTES. Since iNOS and COX-2 are key enzymes responsible for NO and PGE2 production, respectively [30], the reduction in their expression following SC treatment suggests that SC inhibits these mediators by suppressing iNOS and COX-2 activity. Collectively, these data support the anti-inflammatory potential of SC in LPS-challenged macrophages.

Additionally, SC prevented phosphorylation of NF-κB, AP-1, and IRF3 and inhibited their nuclear translocation, indicating suppression of TLR4-linked inflammatory signaling. Because NF-κB activation is regulated by the IKK complex and subsequent IκB degradation [31], we examined upstream components and observed decreased levels of phosphorylated IKKα/β, IκBα, and p65 following SC treatment. SC also reduced nuclear p65 accumulation, suggesting inhibition of the TLR4/IKKα/β/NF-κB pathway. TLR4 activation also stimulates MAPKs (p38, ERK, JNK), leading to AP-1 activation [32]. Our results showed that SC inhibited the phosphorylation of these MAPKs, decreased phosphorylated c-Jun, and reduced its nuclear translocation, indicating suppression of the TLR4/MAPK/c-Jun signaling axis. Furthermore, since TBK1 phosphorylates IRF3, enabling its dimerization and nuclear entry [33], the observed reduction in phosphorylated TBK1 and IRF3 levels, along with reduced nuclear IRF3, demonstrates that SC also blocks the TLR4/TBK1/IRF3 pathway.

This study has limitations. First, the in vitro analysis of inflammatory mediators involved a small sample size (n = 4), as disruptions in ELISA kit supply during the COVID-19 pandemic prevented timely repetition. Second, SC's effects on lung function parameters—such as airway resistance—in the LPS-induced ALI model remain to be evaluated. Third, adoptive macrophage transfer experiments are needed to more clearly define how SC suppresses macrophage-mediated inflammation. These investigations will be integrated into future studies to further validate SC's therapeutic potential for pulmonary inflammatory diseases.

Conclusion

Overall, our findings demonstrate that SC significantly attenuates inflammatory responses in both LPS-induced ALI mice and LPS-stimulated RAW264.7 macrophages. This protective effect appears to involve inhibition of TLR4-mediated signaling cascades, resulting in reduced secretion of inflammatory mediators by immune cells such as macrophages. These results offer pharmacological support for the application of SC in treating pulmonary inflammation associated with various respiratory disorders.

Abbreviations

SC, Sichen formula; ALI, acute lung injury; LPS, lipopolysaccharide; BALF, bronchoalveolar lavage fluid; ELISA, enzyme-linked immunosorbent assay; ARDS, acute respiratory distress syndrome; TLR, toll-like receptor; IκB, inhibitor of nuclear factor-κB; NF-κB, nuclear factor-κB; IKK, IκBα kinase; JNK, c-Jun N-terminal kinase; MAPK, mitogen-activated protein kinase; ERK, extracellular signal-regulated kinase; AP-1, activator protein 1; TBK, TANK-binding kinase; IRF, interferon regulatory factor; MTT, 3-[4,5-dimethylthiazol-2-yl]-2,5-diphenyl tetrazolium bromide; FBS, fetal bovine serum; DMEM, Dulbecco's Modified Eagle Medium; TNF-α, tumor necrosis factor-α; IL, interleukin; MIP-1α, macrophage inflammatory protein 1α; MCP-1, monocyte chemoattractant protein 1; RANTES, regulated upon activation normal T cell expressed and secreted factor; PGE2, prostaglandin E2; COX-2, cyclooxygenase-2; iNOS, inducible nitric oxide synthase; Ig, immunoglobulin; DAPI, 4′,6-diamidino-2-phenylindole; SEM, standard error of the mean.

Acknowledgments: We thank Prof. Gan Luo for his work on molecular docking simulation.

Conflict of Interest: None

Financial Support: This work was supported by the Key Science and Technology Research Projects of Tibet Autonomous Region of China (XZ201801-GA-16).

Ethics Statement: All the animal studies followed the National Institutes of Health Guide for the Care and Use of Laboratory Animals and approved by the Animal Care and Welfare Committee of Beijing University of Chinese Medicine [Certificate No. BUCM-4-2021031103-1048].

References

1. Matthay MA, Zemans RL, Zimmerman GA, Arabi YM, Beitler JR, Mercat A, et al. Acute respiratory distress syndrome. Nat Rev Dis Primers. 2019;5(1):18. doi:10.1038/s41572-019-0069-0
2. Ashbaugh D, Bigelow DB, Petty T, Levine B. Acute respiratory distress in adults. Lancet. 1967;290(7511):319–23. doi:10.1016/S0140-6736(67)90168-7
3. Butt Y, Kurdowska A, Allen TC. Acute lung injury: a clinical and molecular review. Arch Pathol Lab Med. 2016;140(4):345–50. doi:10.5858/arpa.2015-0519-RA
4. Bellani G, Laffey JG, Pham T, Fan E, Brochard L, Esteban A, et al. Epidemiology, patterns of care, and mortality for patients with acute respiratory distress syndrome in intensive care units in 50 countries. JAMA. 2016;315(8):788-800. doi:10.1001/jama.2016.0291. Erratum in: JAMA. 2016 Jul 19;316(3):350. doi:10.1001/jama.2016.6956. Erratum in: JAMA. 2016 Jul 19;316(3):350. doi:10.1001/jama.2016.9558. PMID: 26903337.
5. Sevransky JE, Levy MM, Marini JJ. Mechanical ventilation in sepsis-induced acute lung injury/acute respiratory distress syndrome: an evidence-based review. Crit Care Med. 2004;32(11):S548–53. doi:10.1097/01.CCM.0000145947.19077.25
6. Villar J, Ferrando C, Martínez D, Ambrós A, Muñoz T, Soler JA, et al. Dexamethasone treatment for the acute respiratory distress syndrome: a multicentre, randomised controlled trial. Lancet Respir Med. 2020;8(3):267-76. doi:10.1016/S2213-2600(19)30417-5. Epub 2020 Feb 7. PMID: 32043986.
7. Levy BD, Serhan CN. Resolution of acute inflammation in the lung. Annu Rev Physiol. 2014;76:467–92. doi:10.1146/annurev-physiol-021113-170408

8. Lee JW, Chun W, Lee HJ, Min JH, Kim SM, Seo JY, et al. The role of macrophages in the development of acute and chronic inflammatory lung diseases. Cells. 2021;10(4):897. doi:10.3390/cells10040897. PMID: 33919784; PMCID: PMC8070705.
9. Lawrence T. The nuclear factor NF-kappaB pathway in inflammation. Cold Spring Harb Perspect Biol. 2009;1(6):a001651. doi:10.1101/cshperspect.a001651. Epub 2009 Oct 7. PMID: 20457564; PMCID: PMC2882124.
10. Carter AB, Monick MM, Hunninghake GW. Both Erk and p38 kinases are necessary for cytokine gene transcription. Am J Respir Cell Mol Biol. 1999;20(4):751–8. doi:10.1165/ajrcmb.20.4.3420
11. Kumar V. Pulmonary innate immune response determines the outcome of inflammation during pneumonia and sepsis-associated acute lung injury. Front Immunol. 2020;11:1722. doi:10.3389/fimmu.2020.01722
12. Ge-Sang CR, Yu RY. Acute toxicity study of tibetan medicine sichen formula. J Med Pharm Chins Minor. 2014;20(10):48. doi:10.16041/j.cnki.cn15-1175.2014.10.029 [in Chinese]
13. Yan LS, Cui S, Cheng BC, Yin XB, Wang YW, Qiu XY, et al. Sichen formula ameliorates lipopolysaccharide-induced acute lung injury via blocking the TLR4 signaling pathways. Drug Des Dev Ther. 2023:297-312.
14. Wang JL, Zhou HY, Dun, Z, Pan, D. Pharmacodynamic research on antitussive effect of Tibet medicine Si Chen Zhi Ke Granule. Chin J Tradit Chin Med Pharm. 2007;22(12):895–8. [in Chinese]
15. Seeliger D, de Groot BL. Ligand docking and binding site analysis with PyMOL and Autodock/Vina. J Comput Aided Mol Des. 2010;24(5):417–22. doi:10.1007/s10822-010-9352-6
16. Tsai CL, Lin YC, Wang HM, Chou TC. Baicalein, an active component of Scutellaria baicalensis, protects against lipopolysaccharide-induced acute lung injury in rats. J Ethnopharmacol. 2014;153(1):197–206. doi:10.1016/j.jep.2014.02.010
17. Luo G, Cheng BC, Zhao H, Fu XQ, Xie R, Zhang SF, et al. Schisandra chinensis lignans suppresses the production of inflammatory mediators regulated by NF-κB, AP-1, and IRF3 in lipopolysaccharide-stimulated RAW264. 7 cells. Molecules. 2018;23(12):3319.
18. Zhang Y, Chi-Yan Cheng B, Xie R, Xu B, Gao XY, Luo G. Re-Du-Ning inhalation solution exerts suppressive effect on the secretion of inflammatory mediators via inhibiting IKKα/β/IκBα/NF-κB, MAPKs/AP-1, and TBK1/IRF3 signaling pathways in lipopolysaccharide stimulated RAW 264.7 macrophages. RSC Adv. 2019;9(16):8912–25. doi:10.1039/C9RA00060G
19. Malik K, Ahmad M, Zhang G, Rashid N, Zafar M, Sultana S, et al. Traditional plant based medicines used to treat musculoskeletal disorders in Northern Pakistan. Eur J Integr Med. 2018;19:17-64.
20. Yue Y, Li Q, Fu Y, Chang J. Stability of chlorogenic acid from artemisiae scopariae herba enhanced by natural deep eutectic solvents as green and biodegradable extraction media. ACS Omega. 2021;6(50):34857–65. doi:10.1021/acsomega.1c05541
21. Asl MN, Hosseinzadeh H. Review of pharmacological effects of Glycyrrhiza sp. and its bioactive compounds. Phytother Res. 2008;22(6):709–24. doi:10.1002/ptr.2362
22. Chen H, Jiang Z. The essential adaptors of innate immune signaling. Protein Cell. 2013;4(1):27–39. doi:10.1007/s13238-012-2063-0
23. Fu K, Xu M, Zhou Y, Li X, Wang Z, Liu X, et al. The Status quo and way forwards on the development of tibetan medicine and the pharmacological research of tibetan materia Medica. Pharmacol Res. 2020;155:104688. doi:10.1016/j.phrs.2020.104688. Epub 2020 Feb 13. PMID: 32061838.
24. Yang S, Yu Z, Wang L, Yuan T, Wang X, Zhang X, et al. The natural product bergenin ameliorates lipopolysaccharide-induced acute lung injury by inhibiting NF-kappaB activition. J Ethnopharmacol. 2017;200:147-55. doi:10.1016/j.jep.2017.02.013. Epub 2017 Feb 10. PMID: 28192201.
25. Zhang X, Huang H, Yang T, Ye Y, Shan J, Yin Z, et al. Chlorogenic acid protects mice against lipopolysaccharide-induced acute lung injury. Injury. 2010;41(7):746-52. doi:10.1016/j.injury.2010.02.029. Epub 2010 Mar 15. PMID: 20227691.
26. Shi JR, Mao LG, Jiang RA, Qian Y, Tang HF, Chen JQ. Monoammonium glycyrrhizinate inhibited the inflammation of LPS-induced acute lung injury in mice. Int Immunopharmacol. 2010;10(10):1235–41. doi:10.1016/j.intimp.2010.07.004
27. Maus U, von Grote K, Kuziel WA, Mack M, Miller EJ, Cihak J, et al. The role of CC chemokine receptor 2 in alveolar monocyte and neutrophil immigration in intact mice. Am J Respir Crit Care Med. 2002;166(3):268-73. doi:10.1164/rccm.2112012. PMID: 12153956.

28. Holness CL, Simmons DL. Molecular cloning of CD68, a human macrophage marker related to lysosomal glycoproteins. Blood. 1993;81(6):1607–13. doi:10.1182/blood.V81.6.1607.1607
29. Jeyaseelan S, Chu HW, Young SK, Freeman MW, Worthen GS. Distinct roles of pattern recognition receptors CD14 and Toll-like receptor 4 in acute lung injury. Infect Immun. 2005;73(3):1754–63. doi:10.1128/IAI.73.3.1754-1763.2005
30. Murakami A, Ohigashi H. Targeting NOX, INOS and COX-2 in inflammatory cells: chemoprevention using food phytochemicals. Int J Cancer. 2007;121(11):2357–63. doi:10.1002/ijc.23161
31. Oeckinghaus A, Hayden MS, Ghosh S. Crosstalk in NF-κB signaling pathways. Nat Immunol. 2011;12(8):695–708. doi:10.1038/ni.2065
32. Yang H, Young DW, Gusovsky F, Chow JC. Cellular events mediated by lipopolysaccharide-stimulated toll-like receptor 4. MD-2 is required for activation of mitogen-activated protein kinases and Elk-1. J Biol Chem. 2000;275(27):20861–6. doi:10.1074/jbc.M002896200
33. Perry AK, Chow EK, Goodnough JB, Yeh WC, Cheng G. Differential requirement for TANK-binding kinase-1 in type I interferon responses to toll-like receptor activation and viral infection. J Exp Med. 2004;199(12):1651–8. doi:10.1084/jem.20040528